

Inefficiency of the block approximation in diploid Probabilistic Cellular Automata

Emilio N.M. Cirillo,¹ Joram L. Vliem,^{2,3} Dirk Schuricht,³ and Cristian Spitoni²

¹*Dipartimento di Scienze di Base e Applicate per l’Ingegneria,
Sapienza Università di Roma, via A. Scarpa 16, I-00161, Roma, Italy.*

²*Institute of Mathematics, University of Utrecht,
Budapestlaan 6, 3584 CD Utrecht, The Netherlands.*

³*Institute for Theoretical Physics Utrecht University,
Princetonplein 5, 3584 CC Utrecht, The Netherlands*

We study a probabilistic cellular automaton obtained as a mixture of the additive elementary rules 60 and 102. We prove that, for any finite periodic lattice and for mixing parameter $\lambda = 1/2$, the system almost surely reaches the absorbing all-zero configuration in finitely many steps. In addition, Monte Carlo simulations indicate as well the presence of a zero-density stationary state in a finite interval around $\lambda = 1/2$. Despite this absorbing behavior, both mean-field and block approximation schemes predict a stationary state with non-zero density. This failure, traced to the additive and mirror symmetries of the deterministic components, highlights a fundamental limitation of finite-block approximation in capturing the global dynamics of probabilistic cellular automata.

I. INTRODUCTION

Probabilistic Cellular Automata (PCA) are a stochastic generalization of deterministic Cellular Automata (CA). They are defined as discrete-time Markov chains whose state space is the product of a finite single-site state space. The cell variables are simultaneously updated according to a single-cell probability distribution which depends on the neighboring cells configuration at the previous time. Despite their simplicity, PCA exhibit an ample variety of dynamical behaviors and are thus considered powerful and useful modelling tools. We refer the interested reader to [1] for a comprehensive introduction to the subject and to [2, 3] for recent applications.

The focus of this paper is on the stationary behavior of a particular class of PCA which are a probabilistic mixture of Elementary Cellular Automata (ECA) that is to say, one-dimensional CA in which the state of a cell, either zero or one, is chosen depending on its previous state and on that of its two neighboring cells [4, 5]. Binary probabilistic mixtures are called *diploid* and have been widely studied in the literature [6–11] not only for their intrinsic interest, but also because some of them encode the evolution rule of very well known paradigmatic PCA models.

In this work we study the diploid PCA obtained as a probabilistic mixture (with mixing parameter λ) of the additive ECA rules 60 and 102 which are left-right reflections of one another (see Table I). Although both rules

are linear over \mathbb{Z}_2 and individually generate Sierpiński-type patterns (see [12]), their mixture exhibits an interesting absorbing-state phenomenon. Monte Carlo simulations indicate the presence of an *inactive* or *zero-density* stationary state in an interval of λ values around $\lambda = 1/2$, separated by two symmetric transition points from a non-zero density regime.

This absorbing behavior stands in sharp contrast to what is predicted by common approximation methods. Both the Mean-Field (MF) and the Block Approximation (BA) with block sizes up to $M = 13$ produce positive stationary densities for all $\lambda \in (0, 1)$, and therefore fail to detect the zero-density stationary state suggested by the simulations and rigorously proven at the symmetric point. A detailed analysis of the BA shows that the block-approximation density $\rho_M(\lambda)$ decays exponentially with M , and an extrapolation to infinite block size yields values compatible with zero near $\lambda = 1/2$. However, the effective block size required to reproduce this behavior is of order $M \approx 38$, far beyond computationally feasible block sizes.

This work has two main objectives. First, as discussed above, we show that the MF and BA schemes fail to capture the transition between the zero-density and positive-density states. Second, we rigorously establish the existence of the zero-density state at $\lambda = 1/2$. To this end, we develop a rigorous argument based on estimating the probability that the dynamics maps an arbitrary configuration to the all-zero configuration within a finite number

of time steps. Our central result is that this probability is strictly positive. In addition, Monte Carlo simulations indicate that the zero-density phase extends to a finite interval around $\lambda = 1/2$.

The remainder of the paper is organized as follows. Section II recalls the definition of diploid PCA and reviews the BA scheme. Section III introduces the diploid mixture of rules 60 and 102, describes its additive properties, and presents numerical simulations. Section IV contains the rigorous proof of absorption for $\lambda = 1/2$, i.e., the all-zero configuration is almost surely reached in finite time. Section V analyses in detail the behavior of MF and BA, including an exponential scaling study of the block-size dependence. Finally, Section VI summarizes the results and outlines future directions.

II. MIXTURE OF ECA AND BLOCK APPROXIMATION

We introduce in brief the probabilistic mixtures of ECA and the BA approach. We refer to [13] for a more detailed discussion and for several examples of applications.

Call $Q = \{0, 1\}$ the *set of states* and $\mathbb{Z}_n = \mathbb{Z}/n\mathbb{Z} = \{0, 1, \dots, n-1\}$ the n cell annulus, with n an integer. The *configuration space* is $X_n = Q^{\mathbb{Z}_n}$. For $x \in X_n$, $\Delta \subset \mathbb{Z}_n$, the restriction of x to Δ is x_Δ . We abuse notation by writing x_i for $x_{\{i\}}$ and call it the *value* of the cell i or the *occupation number* of the cell i .

Given the map $F : X_n \rightarrow X_n$, the CA associated with F is the collection of the sequences of configurations ζ^t , with $t \in \mathbb{N}_0$ such that $\zeta^t = F(\zeta^{t-1})$. The sequence ζ^t such that $\zeta^0 = x_0 \in X_n$ is the *trajectory* of the CA with *initial condition* x_0 .

In ECA cell states are updated according to the state of the *neighborhood* $I_i = \{i-1, i, i+1\}$ of the cell $i \in \mathbb{Z}_n$. Note that, due to the periodicity of \mathbb{Z}_n , the neighborhood of the origin is $I_0 = \{n-1, 0, 1\}$. Thus, given a function $f : Q^3 \rightarrow Q$, called *local rule*, the associated ECA is the CA defined by the map $F : X_n \rightarrow X_n$ such that $(F(x))_i = f(x_{I_i})$, for any $i \in \mathbb{Z}_n$ and $x \in X_n$.

The 256 possible ECA [12] are identified by the integer number

$$\begin{aligned} W = & f(1, 1, 1) \cdot 2^7 + f(1, 1, 0) \cdot 2^6 + f(1, 0, 1) \cdot 2^5 \\ & + f(1, 0, 0) \cdot 2^4 + f(0, 1, 1) \cdot 2^3 + f(0, 1, 0) \cdot 2^2 \\ & + f(0, 0, 1) \cdot 2^1 + f(0, 0, 0) \cdot 2^0 \end{aligned} \quad (1)$$

belonging to $\{0, \dots, 255\}$. The coefficients of the above expansion provide the binary representation of the number W and are sometimes used to denote the ECA. Note that for the given ECA W , the *conjugate under left-right reflection* rule is obtained by exchanging $f(1, 1, 0)$ with $f(0, 1, 1)$ and $f(1, 0, 0)$ with $f(0, 0, 1)$.

PCA are defined as Markov chains ζ^t , with $t \in \mathbb{N}_0$, on X_n with transition matrix from state x to y

$$p(x, y) = \prod_{i \in \mathbb{Z}_n} p_i(y_i|x), \quad (2)$$

with the *one-site updating probability* $p_i(\cdot|x)$ being a probability distribution on Q parameterized by the configuration x . Thus, at each time all the cells are updated simultaneously and independently. We denote with \mathbb{P}_x the probability associated with the chain started at x and, thus, $\mathbb{P}_x(\zeta^t = y)$ (resp. $\mathbb{P}_x(\zeta^t \in Y)$) is the probability that the chain started at x is at time t in the configuration y (resp. in the set of configurations $Y \subset X_n$).

PCA can be defined as probabilistic mixtures of ECA by choosing

$$p_i(y_i|x) = y_i \phi(x_{I_i}) + (1 - y_i)[1 - \phi(x_{I_i})], \quad (3)$$

where $\phi : Q^3 \rightarrow [0, 1]$, which can be interpreted as the probability to set the cell to one, is defined as

$$\phi = \sum_{r=1}^m \xi_r f_r, \quad (4)$$

with m a positive integer, $\xi_r \in [0, 1]$ such that $\xi_1 + \dots + \xi_m = 1$ and f_1, \dots, f_m are m local rules. The following interpretation is in order: at each time and for each cell in \mathbb{Z}_n one chooses at random one integer r in $\{1, \dots, m\}$ with probabilities ξ_1, \dots, ξ_m and performs the updating with the rule f_r based on the neighborhood configuration at time $t-1$. Indeed, with this algorithm the probability to set the cell to 1 at time t is the sum of the ξ_r such that f_r , computed in the neighborhood configuration at time $t-1$, is one.

The case $m = 2$ has been widely studied in the literature [6, 13–17]: the probabilistic mixtures of ECA are called *diploid* and (4) simplifies to

$$\phi = (1 - \lambda)f_1 + \lambda f_2, \quad (5)$$

with $\lambda \in [0, 1]$.

We will study the possibility for PCA to exhibit stationary behaviors. For a generic probability measure μ on X_n we define the density as the spatially averaged

occupation number

$$\delta_\mu := \frac{1}{n} \sum_{i \in \mathbb{Z}_n} \mu(x_i = 1). \quad (6)$$

If μ is translation invariant, then $\delta_\mu = \mu(x_0 = 1)$. We will call *density* the quantity δ_μ . Moreover, we shall also use

$$\delta_x = \frac{1}{T} \sum_{t=1}^T \frac{1}{n} \sum_{i \in \mathbb{Z}_n} \zeta_i^t, \quad (7)$$

as its empirical estimate in Monte Carlo simulations. The estimate can be improved by starting to average from a suitable thermalization time and sampling the dynamics not at each time but at times separated by a suitable decorrelation time. We want to stress that in the numerical simulations we will always initialize the PCA from an i.i.d. Bernoulli product measure on X_n . Since the update rule is the same at every site, the Markov evolution commutes with spatial translations; hence the distribution of ζ_i^t is translation invariant for every $t \geq 0$. In particular, $\mathbb{E}[\zeta_i^t]$ does not depend on i , and the expected density can be identified with $\mathbb{E}[\zeta_0^t]$.

Block approximations of the stationary measure have been shown to be reliable in several studies, see, e.g., [13, 18] and references therein. We shortly recall the main ideas, slightly modifying the notation with respect to the one adopted in [13]: let a *block* be a sequence of contiguous cells and denote $B_{i,m}$ the m -cell block $\{i, i+1, \dots, i+m-1\}$, with $i \in \mathbb{Z}_n$ and $1 \leq m \leq n-i$; recall \mathbb{Z}_n is an annulus. Note that the neighborhood I_i defined above is nothing but the block $B_{i-1,3}$. Thus, given z a configuration on $B_{i,m}$ we write

$$\begin{aligned} P_x(\zeta_{B_{i,m}}^t = z) &= \sum_{y \in Q^{B_{i-1,m+2}}} \prod_{k \in B_{i,m}} p_k(z_k | y) P_x(\zeta_{B_{i-1,m+2}}^{t-1} = y). \end{aligned} \quad (8)$$

Now, let ϱ be the stationary distribution and abuse the notation by writing

$$\varrho(z) = \sum_{y \in X_n : y_{B_{i,m}} = z} \varrho(y) \quad (9)$$

for any $z \in Q^{B_{i,m}}$. Thus, by exploiting periodic boundary conditions and translation invariance, from (8) we get

$$\varrho(z) = \sum_{y \in Q^{B_{0,m+2}}} \prod_{k \in B_{1,m}} p_k(z_k | y) \varrho(y) \quad (10)$$

for any $z \in Q^{B_{1,m}}$. We remark that the left-hand side of the equation above contains the 2^m values of the stationary probability of the configurations on the m -block $B_{1,m}$. Instead, the right-hand side is written in terms of the 2^{m+2} values of the stationary probability of the configurations on the $(m+2)$ -block $B_{0,m+2}$.

The M -cell BA of the stationary measure consists in setting M as the maximal block size and rewriting (10) for the measure on the M -cell block with the $M+2$ -cell measures appearing on the right-hand side approximated by combinations of probabilities associated with smaller blocks.

A very smart approximation is provided by the local structure scheme based on the so-called Bayes' rule for BA [18–20], namely,

$$\varrho(x_1 x_2) \approx \varrho(x_1) \varrho(x_2), \quad (11)$$

and, for $m \geq 3$,

$$\varrho(x_1 \dots x_m) \approx \frac{\varrho(x_1 \dots x_{m-1}) \varrho(x_2 \dots x_m)}{\varrho(x_2 \dots x_{m-1})}. \quad (12)$$

In the case in which the denominator vanishes, we assume $\varrho(x_1 \dots x_m) = 0$.

This approximation ensures that the consistency property of block measures is satisfied, that is to say, the probability of smaller blocks can be computed by considering the marginal of larger blocks measure, by integrating out either the left-hand or the right-hand cell variable, more precisely,

$$\varrho(x_1 \dots x_m) = \sum_{y \in Q} \varrho(y x_1 \dots x_m) = \sum_{y \in Q} \varrho(x_1 \dots x_m y),$$

with $x_1, \dots, x_m \in Q$. This allows to solve equations (10)–(12) using the recursive scheme proposed in [21] within the framework of the cluster variation method and called the natural iteration method. The cluster variation method has been widely applied in the context of the statistical mechanics of lattice spin systems and can be considered a generalization of the MF and Bethe approximations of the stationary density matrix. It has proven to be extremely powerful in detecting the existence of phase transitions, predicting their order and their location in the parameter space, and computing correlation functions; see, e.g., [22–24].

More specifically, the initial M -block probabilities are chosen, and then, at each step of the iteration, the $(m-1)$ -block probabilities are computed via symmetrized marginalization (half of the sum of the left and right marginals). Next, the equations (10)–(12) are employed

to compute the new M -block probabilities. This algorithm is repeated until a fixed point is reached. In general, we fix an *a priori* precision of 10^{-8} for the L^2 -norm of the M -block probabilities.

For more explicit expressions of the iterative equation in the cases $M = 3, 5, 7, 9$ we refer the interested reader to [13]. Here we note that, from (11) and (12) we get

$$\varrho(x_1 x_2 x_3) \approx \frac{\varrho(x_1 x_2) \varrho(x_2 x_3)}{\varrho(x_2)} \approx \varrho(x_1) \varrho(x_2) \varrho(x_3), \quad (13)$$

so that the 1-BA is nothing but the MF approximation.

Several papers (e.g., [13, 18, 25]) have exploited the remarkable ability of the BA to reproduce accurately the structure of the stationary measures of PCA. For instance, the paper [13] approached this problem not only in the diploid case, but also for a mixture of three local rules resulting in a PCA which exhibits a double transition as a function of the mixing parameter. We also refer to the papers discussed in the introductory part of this note.

III. A HIGHLY SYMMETRIC DIPLOID

In this paper we are interested in the diploid obtained as a mixture of the ECA 60 and 102, and show that, due to its highly symmetric character, the BA, at least at the order that we have considered, is not able to capture the existence of the zero-density stationary state. The behavior of the diploid is described in Table I.

	111	110	101	100	011	010	001	000
60	0	0	1	1	1	1	0	0
102	0	1	1	0	0	1	1	0

TABLE I. Deterministic dynamics of ECA 60 and 102. The rule is reported in the first column. The following columns provide the update of the central site of the neighborhood reported in the first row.

The two rules are conjugate to each other under left-right reflection. In Figure 1 the evolution of the two deterministic rules is shown: both rules produce the *Sierpiński triangle* patterns from a single active cell. Moreover, they correspond to well-known Boolean functions: ECA 60 implements the local rule $f_1(a, b, c) = a \oplus b$, while ECA 102 implements $f_2(a, b, c) = b \oplus c$, where \oplus denotes addition modulo 2 (XOR operator). This formal correspondence allows us to view these cellular automata as spatially distributed XOR functions. Furthermore, both rules are

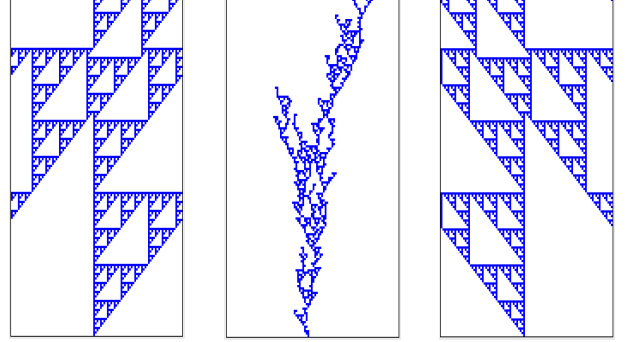


FIG. 1. The left and right panels report, respectively, the evolution up to time 150 of the ECA 60 and 102 on a 100-cell periodic lattice; the central panel reports the diploid mixture with parameter $\lambda = 1/2$. Unit squares represent cells in state one. In the initial configuration the state of all the cells is zero, but for the one at the center of the lattice. In the plot the time runs upwards.

additive: for any two configurations $x, y \in \{0, 1\}^{\mathbb{Z}_n}$, their sum (bit-wise XOR) evolves linearly:

$$A(x \oplus y) = Ax \oplus Ay,$$

where we denote by $A : X_n \rightarrow X_n$ the linear operator over \mathbb{Z}_2 associated for instance to the deterministic update of ECA 60, defined by:

$$(Ax)_i := x_{i-1} \oplus x_i, \quad i \in \mathbb{Z}_n, \quad (14)$$

where the indices are taken modulo n . The linearity allows explicit computation of their space-time evolution and leads to characteristic diagonal stripe patterns. Moreover, on finite rings of odd length, both ECA 60 and ECA 102 are invertible, hence the corresponding dynamics are *reversible*: each configuration has a unique predecessor under the same rule.

In Figure 2 we show the time evolution of the diploid with mixing parameter $\lambda = 1/2$, and we observe that after 1080 iterations the system reaches the absorbing state with zero density. We consider now the late-time behavior of the diploid with a general λ , see (5), with f_1 the rule ECA 60 and f_2 the rule ECA 102. The Monte Carlo simulation for the density is reported in Figure 3: the simulation was performed on the lattice with $n = 10^5$ cells, for a total time of 10^5 . The density was estimated using (7) with 10^4 as thermalization time and 10^2 as decorrelation time. According to the Monte Carlo results, the system undergoes two transitions between a zero and non-zero density stationary state, with a finite

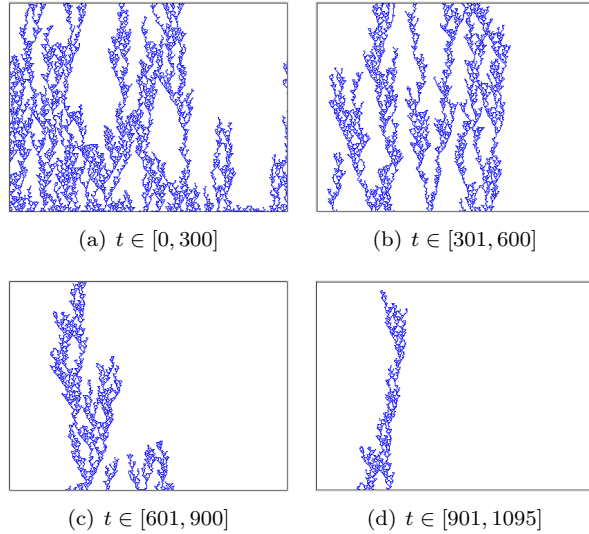


FIG. 2. Time evolution of the diploid with 400 cells, mixture of rules 60 and 102, with parameter $\lambda = 1/2$. The initial configuration is a realization of a Bernoulli distribution of cells with parameter 1/2. The time evolves upwards (a) $t \in [0, 300]$ (b) $t \in [301, 600]$ (c) $t \in [601, 900]$ (d) $t \in [901, 1095]$. At time $t = 1080$ the zero-density state is reached.

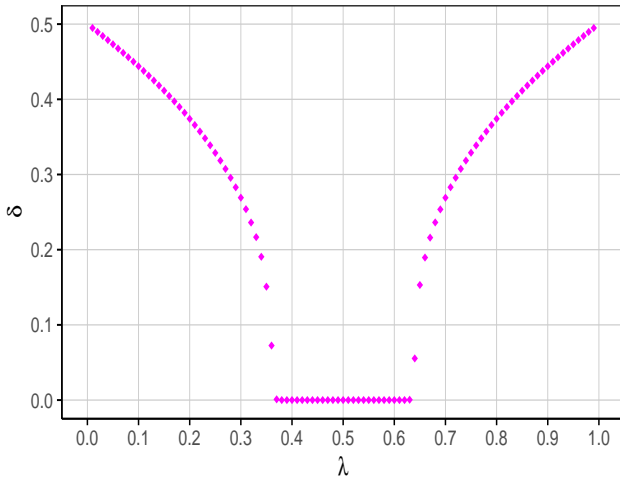


FIG. 3. Density as function of the mixing parameter λ computed via Monte Carlo simulations for a lattice with $n = 10^5$. The thermalization and decorrelation times were 10^4 and 10^2 respectively.

zero-density region in between. The presence of two transition points (λ_c^l and λ_c^r), symmetric with respect to 1/2, is an obvious consequence of the left-right symmetry of the model. In our simulation we have $\lambda_c^l \in (0.37, 0.38)$ and $\lambda_c^r \in (0.62, 0.63)$.

IV. RIGOROUS RESULTS FOR THE BALANCED CASE

We consider here the diploid mixture of ECA 60 and 102 with $\lambda = 1/2$ (see Figure 2 for a realization of a path reaching the stationary absorbing state with zero density), whose relaxation towards the stationarity density can be studied rigorously. This diploid can indeed be written as:

$$\zeta_i^{t+1} = \begin{cases} \zeta_{i-1}^t \oplus \zeta_i^t & \text{if } \zeta_{i-1}^t = \zeta_{i+1}^t \\ \eta_{i,t+1} & \text{if } \zeta_{i-1}^t \neq \zeta_{i+1}^t \end{cases} \quad (15)$$

where $\eta_{i,t+1} \stackrel{i.i.d.}{\sim} \text{Ber}(1/2)$. In other words, for $\lambda = 1/2$ at each site and time step, if the two outer neighbors are equal, the update acts deterministically, $\zeta_i^{t+1} = \zeta_{i-1}^t \oplus \zeta_i^t$; if the two outer neighbors differ, the site updates randomly, $\zeta_i^{t+1} = \eta_{i,t+1}$ with $\eta_{i,t+1} \sim \text{Ber}(1/2)$.

We will prove that, on a finite periodic lattice, the all-zero absorbing configuration $\mathbf{0}$ is reached almost surely in finitely many steps. Using the fact that the deterministic sites D_t (see below) evolve according to the XOR rule and that to the complementary sites F_t are assigned random bits, we will show that there exists a positive-probability sequence of realizations of the Bernoulli variables driving the system to the absorbing state $\mathbf{0}$ in finitely many steps. Our goal is to show that there exists a positive-probability sequence of realizations of Bernoulli variables driving the system to the absorbing state $\mathbf{0}$.

For any fixed t we define the sets:

$$D_t := \{i \in \mathbb{Z}_n : \zeta_{i-1}^t = \zeta_{i+1}^t\}, \quad F_t := \mathbb{Z}_n \setminus D_t. \quad (16)$$

A configuration $y \in X_n$ is called *forbidden* if there exists a site $i \in \mathbb{Z}_n$ such that $(y_{i-1}, y_i, y_{i+1}) \in \{(101), (010)\}$, otherwise it is called *admissible*. With abuse of language, we also call a triple *admissible* if it differs from 101 and 010.

We give now a sketch of the structure of the proof. The first observation (Lemma 1) is that a pair of deterministic sites (i.e., belonging to D_t) in a triple can never produce 010 or 101 under the PCA update. The second ingredient is an admissible-triple construction on any finite interval (Lemma 2): we show that it is possible to choose the Bernoulli variables such that in one time step the evolved configuration is admissible. The third ingredient is a local cleaning principle (Lemma 3): on any interval where all triples are admissible, setting all Bernoulli random variables to zero cleans the entire interval to zero

in one step. Using these tools, we then perform a four-step construction. In the first step, we apply Lemma 2 at time t to the large bulk interval $\{1, \dots, n-2\}$ to ensure that all triples with centers $\{2, \dots, n-3\}$ are admissible at time $t+1$. In the second step, Lemma 3 is used to force all bulk spins $\{2, \dots, n-3\}$ to zero at time $t+2$. The only non-zero sites may lie in the four-site boundary block $\{n-2, n-1, 0, 1\}$. At this point the boundary block has the form $(0, a, b, c, d, 0)$. This block is handled by a four-site boundary lemma (Lemma 4), which observes that the six-site boundary window $(0, a, b, c, d, 0)$ is itself an interval with fixed zero boundaries and can therefore be treated by another application of Lemma 2. This yields admissibility of all triples at time $t+3$. Finally, one last application of Lemma 3 forces the entire configuration to zero at time $t+4$. Altogether, this shows that $\mathbf{0}$ is reachable in at most four steps with strictly positive probability, establishing Theorem 1.

We now prove the lemmas needed for the four-step absorption scheme.

Lemma 1. *Consider the evolved configuration ζ^t at time t and the site $i \in \mathbb{Z}_n$. If at least two of the sites $i-1, i, i+1$ belong to D_t , then, for every choice of the Bernoulli variables at time $t+1$, the triple $(\zeta_{i-1}^{t+1}, \zeta_i^{t+1}, \zeta_{i+1}^{t+1})$ is admissible.*

Proof. Assume that at least two of the sites $(i-1, i, i+1)$ are deterministic at time t . Due to the left-right symmetry, there are only three possible configurations of deterministic sites. For each of them, the deterministic updates impose a forced algebraic relation among the components of the triple $(\zeta_{i-1}^{t+1}, \zeta_i^{t+1}, \zeta_{i+1}^{t+1})$, independently of the Bernoulli variables. These relations are summarized in Table II. In all three cases, the forced relation is incompatible with the patterns 010 and 101: the first two cases force equality of two adjacent entries, while the third forces inequality of the two outer entries, whereas both forbidden patterns require $\zeta_{i-1}^{t+1} \neq \zeta_i^{t+1} = \zeta_{i+1}^{t+1}$ or $\zeta_{i-1}^{t+1} = \zeta_{i+1}^{t+1} \neq \zeta_i^{t+1}$.

If all three sites $i-1, i, i+1$ belong to D_t , then one of the first two cases of Table II applies. We briefly justify the forced relations reported in Table II. If $\{i-1, i\} \subseteq D_t$, then $\zeta_{i-2}^t = \zeta_i^t$ and the deterministic updates give

$$\zeta_{i-1}^{t+1} = \zeta_{i-2}^t \oplus \zeta_{i-1}^t = \zeta_i^t \oplus \zeta_{i-1}^t = \zeta_i^{t+1},$$

so the first two entries of the triple coincide. The case $\{i, i+1\} \subseteq D_t$ is completely analogous by left-right symmetry. Finally, if $\{i-1, i+1\} \subseteq D_t$ and $i \in F_t$, then

$$\zeta_{i-1}^{t+1} = \zeta_i^t \oplus \zeta_{i-1}^t, \quad \zeta_{i+1}^{t+1} = \zeta_i^t \oplus \zeta_{i+1}^t,$$

Deterministic sites at time t	Forced relation
$\{i-1, i\} \subseteq D_t$	$\zeta_{i-1}^{t+1} = \zeta_i^{t+1}$
$\{i, i+1\} \subseteq D_t$	$\zeta_i^{t+1} = \zeta_{i+1}^{t+1}$
$\{i-1, i+1\} \subseteq D_t, i \in F_t$	$\zeta_{i-1}^{t+1} \neq \zeta_{i+1}^{t+1}$

TABLE II. Forced algebraic relations on the updated triple $(\zeta_{i-1}^{t+1}, \zeta_i^{t+1}, \zeta_{i+1}^{t+1})$ when at least two sites among $\{i-1, i, i+1\}$ are deterministic at time t . Each relation excludes the triples 010 and 101, independently of the Bernoulli variables.

and since $i \in F_t$ implies $\zeta_{i-1}^t \neq \zeta_{i+1}^t$, XOR with the same bit ζ_i^t preserves inequality, yielding $\zeta_{i-1}^{t+1} \neq \zeta_{i+1}^{t+1}$. In all cases, the resulting relations are incompatible with the forbidden triples 010 and 101. \square

Lemma 2. *Fix $n \geq 5$ and consider the evolved configuration ζ^t . Consider the interval*

$$I := \{1, 2, \dots, n-2\} \subset \mathbb{Z}_n.$$

Then there exists a choice of the Bernoulli variables at time $t+1$ such that all triples $(\zeta_{i-1}^{t+1}, \zeta_i^{t+1}, \zeta_{i+1}^{t+1})$ are admissible for every $i \in \{2, \dots, n-3\}$.

Proof. Let $I := \{1, 2, \dots, n-2\}$. We construct the variables y_1, \dots, y_{n-2} sequentially from the left to the right.

Starting from $i = 1$, we distinguish two cases. If $1 \in D_t$, set $y_1 := \zeta_0^t \oplus \zeta_1^t$. For $1 \in F_t$, choose y_1 arbitrarily (e.g., $y_1 := 0$).

If $i \in \{2, 3, \dots, n-2\}$, we define y_i by:

$$y_i := \begin{cases} \zeta_{i-1}^t \oplus \zeta_i^t, & \text{if } i \in D_t, \\ y_{i-1}, & \text{if } i \in F_t. \end{cases}$$

For each $i \in \{3, 4, \dots, n-2\}$, we show that the triple (y_{i-2}, y_{i-1}, y_i) centered at $i-1$ is admissible; this will imply the claim.

Fix $i \in \{3, \dots, n-2\}$ and consider the triple (y_{i-2}, y_{i-1}, y_i) . We distinguish three cases.

Case 1: $i \in F_t$. Then $y_i = y_{i-1}$ by the algorithm, hence the last two entries of the triple coincide. Therefore, the triple is admissible.

Case 2: $i \in D_t, i-1 \in F_t$. Therefore, the algorithm set $y_{i-1} = y_{i-2}$, so that the first two entries of the triple centered at $i-1$ coincide. Hence, it is admissible.

Case 3: $i \in D_t, i-1 \in D_t$. Thus, by Lemma 1 the triple centered at $i-1$ is admissible. \square

Remark 1. We would like to stress that locally we can easily prove that at every site i there exists at least one choice of the local Bernoulli variable that makes the triple centered at i admissible at time $t+1$.

Fix, indeed, a site $i \in \mathbb{Z}_n$. Suppose that, at time $t+1$, the triple $(\zeta_{i-1}^{t+1}, \zeta_i^{t+1}, \zeta_{i+1}^{t+1})$ were equal to 010 or 101 with probability 1 over the randomness at time t . Then each of its three coordinates must be deterministically fixed by the update rule (15). For instance, if the triple is almost surely 010, then necessarily

$$\zeta_{i-1}^{t+1} = 0, \quad \zeta_i^{t+1} = 1, \quad \zeta_{i+1}^{t+1} = 0.$$

Examining the update rule, this implies:

1. the site $i-1$ must be deterministic at time t , and its neighbours satisfy $(\zeta_{i-2}^t, \zeta_i^t) \in \{(0,0), (1,1)\}$;
2. the site i must also be deterministic at time t , but its neighbours must satisfy $(\zeta_{i-1}^t, \zeta_{i+1}^t) \in \{(0,1), (1,0)\}$;
3. similarly $i+1$ must satisfy $(\zeta_i^t, \zeta_{i+2}^t) \in \{(0,0), (1,1)\}$.

These conditions are incompatible: from the first item we obtain $\zeta_{i-1}^t = \zeta_i^t$, while from the second item we require $\zeta_{i-1}^t \neq \zeta_i^t$. Thus the preimage of a triple which is almost surely 010 (or 101) is empty.

However, this local argument does not imply Lemma 2, since it does not guarantee that all triples can be made admissible simultaneously. Indeed, triples overlap, so the admissible choices at different sites may interact. Lemma 2 shows indeed that, despite these global compatibility constraints, a full assignment of the Bernoulli variables making every triple admissible always exists.

Lemma 3. Assume $\zeta^t = x$, with x a configuration with all admissible triples. If we choose $\eta_{j,t+1} = 0$ whenever $j \in F_t$, then

$$\zeta^{t+1} = \mathbf{0}.$$

Proof. If $j \in D_t$, admissibility forces $x_{j-1} = x_j = x_{j+1}$, and hence $\zeta_j^{t+1} = x_{j-1} \oplus x_j = 0$. If $j \in F_t$, setting $\eta_{j,t+1} = 0$ gives $\zeta_j^{t+1} = 0$ by definition. \square

Lemma 4. Let $z \in X_n$ be a configuration such that $z_i = 0$ for all $i \in \{2, 3, \dots, n-3\}$. If $\zeta^t = z$, then there exists a choice of Bernoulli variables at time $t+1$ such that the evolved configuration ζ^{t+1} is such that all the triples centered at $n-2, n-1, 0, 1$ are admissible.

Proof. Consider the six-site block

$$(0, a, b, c, d, 0) =: (z_{n-3}, z_{n-2}, z_{n-1}, z_0, z_1, z_2).$$

Regard it as an interval of size 6 and apply Lemma 2 to $I = \{n-3, n-2, n-1, 0, 1, 2\}$ with fixed boundaries $z_{n-3} = z_2 = 0$. Lemma 2 guarantees that all triples centered not in the boundary are admissible. \square

Theorem 1. For any $n \geq 5$, consider the configuration ζ^t at time t , then there exists a choice of the Bernoulli variables over the next four times such that $\zeta^{t+4} \equiv \mathbf{0}$. In other words, the all-zero configuration is reachable with strictly positive probability in four steps.

Proof. We provide a proof organized in four steps.

Step 1 (interval admissibility on the bulk). Apply Lemma 2 to the interval $\{1, 2, \dots, n-2\}$, and choose the Bernoulli variables so that ζ^{t+1} is admissible on all triples centered at $\{2, \dots, n-3\}$.

Step 2 (local cleaning of the bulk). Choose $\eta_{i,t+2} = 0$ for all $i \in \{2, \dots, n-3\} \cap F_{t+1}$. By Lemma 3, this yields

$$\zeta_i^{t+2} = 0 \quad \text{for all } i \in \{2, \dots, n-3\}.$$

Step 3 (boundary cleaning). The configuration ζ^{t+2} has the form

$$(0, a, b, c, d, 0) \quad \text{on } \{n-3, n-2, n-1, 0, 1, 2\},$$

and zero otherwise. Apply Lemma 4 at time $t+2$. This yields ζ^{t+3} has only admissible triples.

Step 4 (global cleaning). Since ζ^{t+3} has only admissible triples, setting all $\eta_{i,t+4} = 0$, for all $i \in F_{t+4}$, yields $\zeta_i^{t+4} = 0$ for all i by Lemma 3. Hence, $\zeta^{t+4} \equiv \mathbf{0}$.

All four random variable assignments have positive probability, therefore the probability of this four-step path to $\mathbf{0}$ is strictly positive. \square

Before stating Theorem 2, we stress that its proof is standard in the theory of finite-state Markov chains. For a Markov chain with a unique absorbing state, if this state is reachable from every other configuration with strictly positive probability, then absorption occurs almost surely in finite time. We nevertheless provide a proof for the sake of completeness and to make explicit the role of Theorem 1 in the almost sure absorption.

Theorem 2. For $\lambda = 1/2$, and $n \geq 5$, the configuration $\mathbf{0}$ is the unique absorbing state of the PCA (15), and it is reached almost surely in finite time from any initial configuration.

Proof. By Theorem 1, for every initial configuration $x \in X_n$ we have

$$\mathbb{P}_x(\zeta^4 = \mathbf{0}) > 0.$$

Since the state space X_n is finite, the minimum of these strictly positive numbers is strictly positive; define

$$\varepsilon := \min_{x \in X_n} \mathbb{P}_x(\zeta^4 = \mathbf{0}) > 0.$$

For $k \geq 0$ set $A_k := \{\zeta^{4k} \neq \mathbf{0}\}$. We claim that for every $x \in X_n$ and every $k \geq 0$:

$$\mathbb{P}_x(A_{k+1}) \leq (1 - \varepsilon) \mathbb{P}_x(A_k). \quad (17)$$

To prove (17), we use the law of total probability with respect to the random variable ζ^{4k} :

$$\mathbb{P}_x(A_{k+1}) = \sum_{y \in X_n} \mathbb{P}_x(A_{k+1} \mid \zeta^{4k} = y) \mathbb{P}_x(\zeta^{4k} = y). \quad (18)$$

If $y = \mathbf{0}$, then we have $\mathbb{P}_x(A_{k+1} \mid \zeta^{4k} = \mathbf{0}) = 0$. If $y \neq \mathbf{0}$, then by the Markov property and time-homogeneity we have:

$$\mathbb{P}_x(A_{k+1} \mid \zeta^{4k} = y) = \mathbb{P}_y(\zeta^4 \neq \mathbf{0}) \leq 1 - \varepsilon.$$

Thus

$$\begin{aligned} \mathbb{P}_x(A_{k+1}) &= \sum_{y \neq \mathbf{0}} \mathbb{P}_x(A_{k+1} \mid \zeta^{4k} = y) \mathbb{P}_x(\zeta^{4k} = y) \\ &\leq (1 - \varepsilon) \sum_{y \neq \mathbf{0}} \mathbb{P}_x(\zeta^{4k} = y). \end{aligned}$$

But $\sum_{y \neq \mathbf{0}} \mathbb{P}_x(\zeta^{4k} = y) = \mathbb{P}_x(\zeta^{4k} \neq \mathbf{0}) = \mathbb{P}_x(A_k)$, so (17) follows. Iterating (17) yields, for all $k \geq 0$,

$$\mathbb{P}_x(A_k) \leq (1 - \varepsilon)^k. \quad (19)$$

Consider now the event that the chain never hits $\mathbf{0}$:

$$\{\tau_{\mathbf{0}} = \infty\} = \{\zeta^t \neq \mathbf{0} \text{ for all } t \geq 0\},$$

where $\tau_{\mathbf{0}}$ is the first hitting time of the configuration $\mathbf{0}$. Since $\mathbf{0}$ is absorbing, if the chain ever hits $\mathbf{0}$ at some time t then it stays there forever, in particular $\zeta^{4k} = \mathbf{0}$ for all k large enough. Equivalently, the chain never hits $\mathbf{0}$ if and only if $\zeta^{4k} \neq \mathbf{0}$ for infinitely many k , that is,

$$\{\tau_{\mathbf{0}} = \infty\} = \limsup_{k \rightarrow \infty} A_k = \bigcap_{m \geq 0} \bigcup_{k \geq m} A_k. \quad (20)$$

Fix $m \geq 0$. From the inclusion

$$\bigcap_{r \geq 0} \bigcup_{k \geq r} A_k \subseteq \bigcup_{k \geq m} A_k,$$

monotonicity of probability gives

$$\mathbb{P}_x(\tau_{\mathbf{0}} = \infty) = \mathbb{P}_x\left(\bigcap_{r \geq 0} \bigcup_{k \geq r} A_k\right) \leq \mathbb{P}_x\left(\bigcup_{k \geq m} A_k\right).$$

Applying the union bound and (19),

$$\mathbb{P}_x\left(\bigcup_{k \geq m} A_k\right) \leq \sum_{k \geq m} \mathbb{P}_x(A_k) \leq \sum_{k \geq m} (1 - \varepsilon)^k = \frac{(1 - \varepsilon)^m}{\varepsilon}.$$

Since the right-hand side tends to 0 as $m \rightarrow \infty$, we conclude that

$$\mathbb{P}_x(\tau_{\mathbf{0}} = \infty) = 0, \quad \text{i.e.} \quad \mathbb{P}_x(\tau_{\mathbf{0}} < \infty) = 1.$$

Thus the hitting time of $\mathbf{0}$ is finite almost surely.

Assume by contradiction that there exists $y \in X_n$, $y \neq \mathbf{0}$, which is also absorbing. Then the chain started from y remains at y forever, so $\mathbb{P}_y(\zeta^4 = \mathbf{0}) = 0$. This contradicts Theorem 1, which implies $\mathbb{P}_y(\zeta^4 = \mathbf{0}) \geq \varepsilon > 0$. Hence $\mathbf{0}$ is the unique absorbing state. \square

V. MEAN FIELD FAILURE AND BLOCK APPROXIMATION INEFFICIENCY

Theorem 2 shows that for the diploid with ECAs 60, 102 with $\lambda = 1/2$, the all-zero configuration is the unique absorbing state of the PCA and is reached almost surely in finite time from any initial condition. Next, we want to move away from $\lambda = 1/2$ and study the extended region with absorbing state. However, we will show that both the MF and the BA have difficulties detecting this absorbing stationary state and the transitions to the finite-density state observed at the left and at the right of $\lambda = 1/2$.

More precisely, if we consider now the MF approximation, it indeed fails completely in detecting the presence of the zero stationary state. In fact, by recalling (5) and Table I, by writing (10) for the 1-cell block $B_{1,1}$ and exploiting the approximation (13), one gets

$$\begin{aligned} \delta = \varrho(1) &= \lambda(1 - \delta)\delta^2 + (1 - \delta)\delta^2 + (1 - \lambda)(1 - \delta)^2\delta \\ &\quad + (1 - \lambda)(1 - \delta)\delta^2 + (1 - \delta)^2\delta + \lambda(1 - \delta)^2\delta, \end{aligned}$$

which, besides the unstable solution $\delta = 0$ (see Figure 4) admits the non-zero stable solution $\delta = 1/2$ for every value of $\lambda \in (0, 1)$. In other words, the MF approximation predicts the existence of both the zero density and the non-zero density solution for every λ , in contrast with the numerical results of Figure 3.

Furthermore, we also approach the problem with the BA and consider the cases $M = 3, 5, 7, 9, 11, 13$. As

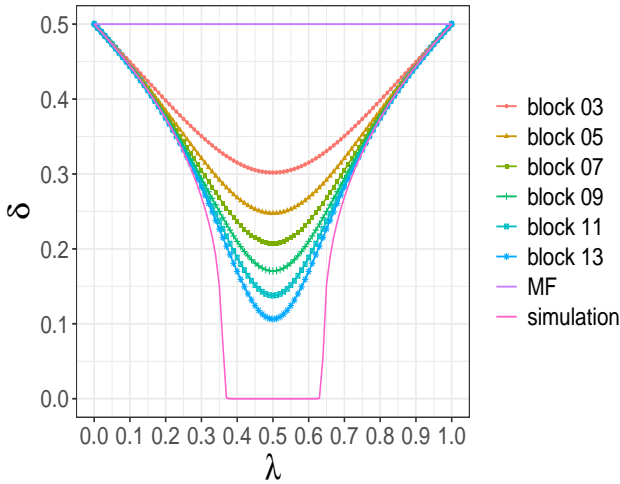


FIG. 4. Density as function of the mixing parameter λ computed via MF, BA of different sizes, and Monte Carlo simulations. For the BA we report the solution found initializing the iterative equations with the 1/2 Bernoulli measure.

shown in Figure 4 the BA greatly improves the MF result, but, nevertheless, it is not able to capture the existence of the transition.

To be more precise, the measure concentrated on the zero block is trivially a solution of the block approximation iterative equations, nevertheless, solving the iterative equations starting from the 1/2 Bernoulli measure the fixed point found in the measure space has positive density for every λ , as reported in Figure 4. Thus, the BA method is not able to predict a transition and provide an estimate of the transition point. We have also explored, without success, different starting points for the iterative equations, looking for smart initial conditions which could, at least for specific values of λ , end up in the measure concentrated on the zero block so that the transition point could be estimated. Summarizing, the measure concentrated on the zero block is a stationary point of the iterative equations, but it appears as a highly unstable fixed point. As soon as the iterations are started from a slightly different point in the block measure space, the algorithm converges to the non-zero density solutions. This behavior is much different from what we observed in several cases, for instance for the diploid considered in [13], for which there exist values of λ such that the measure concentrated on zero becomes a stable fixed point of the iterative equations providing a clear strategy to estimate the transition point.

To further analyze this behavior, in Figure 5 we show how the block approximation $\rho_M(\lambda)$ depends on the

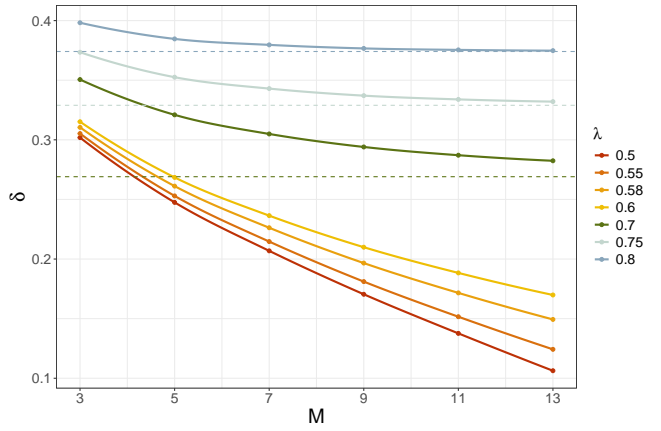


FIG. 5. Decay of the density as function of the size M of the BA for different λ . The dashed lines denote the corresponding asymptotic densities of the Monte Carlo simulations. For large λ the BA agrees with the simulations already at $M = 13$, while it is off in the region of the zero-density absorbing state.

block size $M \in \{3, 5, 7, 9, 11, 13\}$ for each fixed value of λ . The sequence is monotone decreasing and appears to converge as M increases, suggesting that the finite-block corrections follow an exponential relaxation. Motivated by this observation, we fit the six values $\rho_M(\lambda)$ with the three-parameter form

$$\rho_M^{(1)}(\lambda) = a(\lambda) e^{-b(\lambda)M} + c(\lambda), \quad (21)$$

where $c(\lambda)$ represents the asymptotic BA that would be obtained in the formal limit $M \rightarrow \infty$. In this fit, $a(\lambda)$ measures the amplitude of the finite-block corrections and $b(\lambda)$ the rate at which these corrections decay. For each λ , the parameters $(a(\lambda), b(\lambda), c(\lambda))$ were determined by nonlinear least squares. To ensure physical consistency of the density, we imposed the natural positivity constraints $a(\lambda) \geq 0$, $b(\lambda) \geq 0$ and $c(\lambda) \geq 0$, preventing the fit from producing unphysical negative densities. The goodness of the fit was quantified using the coefficient of determination

$$R^2(\lambda) = 1 - \frac{\sum_M \left(\rho_M^{(1)}(\lambda) - a(\lambda) e^{-b(\lambda)M} - c(\lambda) \right)^2}{\sum_M \left(\rho_M^{(1)}(\lambda) - \overline{\rho^{(1)}(\lambda)} \right)^2},$$

where $\overline{\rho^{(1)}(\lambda)}$ is the mean of the six values $\rho_M^{(1)}(\lambda)$. The constrained exponential fit achieves an excellent description of the data: for all $\lambda \geq 0.01$ we find

$$0.93 \leq R^2(\lambda) \leq 0.9995,$$

with $R^2(\lambda) > 0.995$ throughout the region of interest around $\lambda = 1/2$. The exponential law (21) therefore

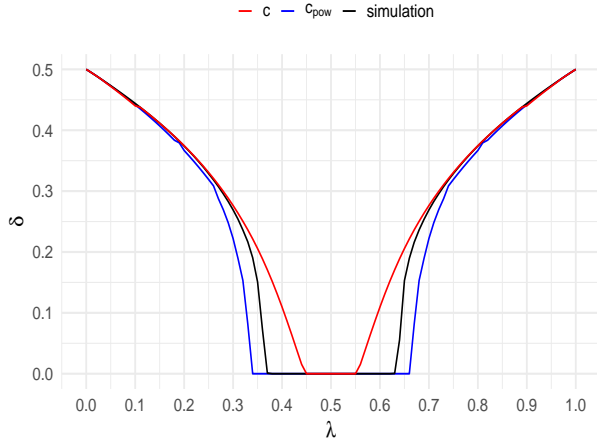


FIG. 6. Coefficients c_{pow} for the power-law model, c for the exponential fit and the values of the Monte Carlo simulations

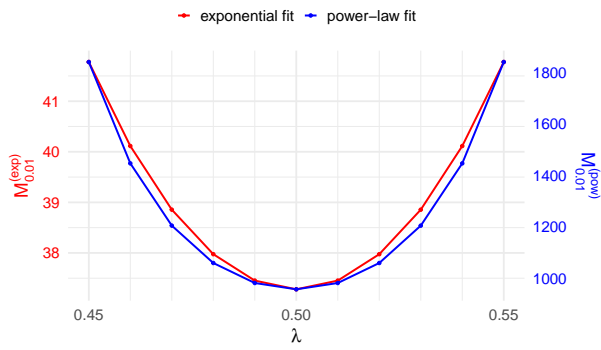


FIG. 7. Effective block size for getting a density as a function of λ , for the exponential and the power-law fits

provides a quantitatively accurate interpolation of the finite-block densities and a reliable extrapolation to $M \rightarrow \infty$.

The resulting asymptotic densities $c(\lambda)$ are shown in Figure 6, together with the Monte Carlo stationary densities (black curve). The agreement is excellent for λ also away from the value $1/2$, confirming that the BA converges smoothly with M . More importantly, in a narrow region around $\lambda = 1/2$ the fitted asymptotic density becomes extremely small and forms a plateau that is statistically compatible with $c(\lambda) = 0$. This is entirely consistent with the exact absorbing behavior of the PCA at $\lambda = 1/2$: although the finite-block values $\rho_M(1/2)$ remain positive for $M \leq 13$, their exponential extrapolation reveals that the infinite-block prediction is a vanishing density.

Figure 7 shows, for each value of the mixing parameter λ , the effective block size $M_{0.01}(\lambda)$ at which the

exponentially fitted BA predicts a density as small as $\rho_M(\lambda) = 0.01$. The value of $M_{0.01}(\lambda)$ is obtained by inverting the constrained exponential fit (21), namely

$$M_{0.01}(\lambda) = \frac{1}{b(\lambda)} \log \left(\frac{a(\lambda)}{0.01 - c(\lambda)} \right),$$

for $c(\lambda) < 0.01$. This plot provides a quantitative measure of how large a block must be before the block-approximation predicts a practically vanishing density. In particular, near $\lambda = 1/2$, the required block size is of the order of $M \approx 38$, much larger than our maximal block size 13 in Figure 4.

However, it is natural to ask whether describing the decay of the block density $\rho(M)$ as an exponential relaxation toward an asymptotic plateau is too restrictive to capture the behavior observed in the diploid dynamics. Hence, in order to include a power-law decay near the critical points, we complement the analysis based on a single-rate exponential decay by considering a power-law parametrization of the block density. For each value of λ and each accessible block size $M \in \{3, 5, 7, 9, 11, 13\}$, we fit the functional form

$$\rho_M^{(2)}(\lambda) = c_{\text{pow}}(\lambda) + a_{\text{pow}}(\lambda) M^{-b_{\text{pow}}(\lambda)}, \quad (22)$$

with $a_{\text{pow}}, b_{\text{pow}}, c_{\text{pow}} \geq 0$. The resulting asymptotic densities c_{pow} are shown in Figure 6, together with the exponential fit and the Monte Carlo stationary densities. We observe that both extrapolation schemes predict the existence of a zero-density region, with the exponential fit (21) underestimating and the power-law (22) overestimating its size.

Finally, we remark that the ability of the BA to detect transition points is restored if one considers a three ECA mixture (i.e., a *triploid*) adding to the 60 and 102 rules the 0 rule, as well. More precisely, one chooses the function ϕ as in (4) with f_1 the zero rule, f_2 the rule 60, and f_3 the rule 102, with $\xi_1 = \epsilon$, $\xi_2 = 1 - \lambda$, and $\xi_3 = \lambda - \epsilon$, so that for $\epsilon = 0$ the original diploid is recovered. Note that $0 \leq \epsilon \leq \lambda \leq 1$.

The MF approximation, again, fails in identifying the transition, indeed the MF equation

$$\begin{aligned} \delta = \varrho(1) = & (\lambda - \epsilon)(1 - \delta)\delta^2 + (1 - \epsilon)(1 - \delta)\delta^2 \\ & + (1 - \lambda)(1 - \delta)^2\delta + (1 - \lambda)(1 - \delta)\delta^2 \\ & + (1 - \epsilon)(1 - \delta)^2\delta + (\lambda - \epsilon)(1 - \delta)^2\delta, \end{aligned}$$

has the solutions $\delta = 0$ and $\delta = (1 - 2\epsilon)/[2(1 - \epsilon)]$ for every value of λ . The second solution is positive for $\epsilon \in [0, 1/2)$, equal to zero for $\epsilon = 1/2$, and negative (that is to say,

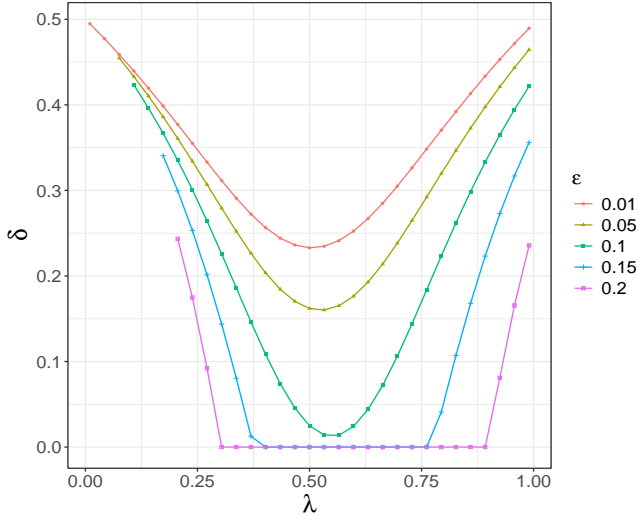


FIG. 8. Density for the three rule mixture as function of $\lambda \in [\epsilon, 1]$ computed via the 5-cell BA for $\epsilon = 0.01$, $\epsilon = 0.05$, $\epsilon = 0.10$, $\epsilon = 0.15$, $\epsilon = 0.20$. We report the solution found initializing the iterative equations with the $1/2$ Bernoulli measure. The corresponding values predicted by the MF approximation are 0.495, 0.474, 0.444, 0.412, and 0.375.

meaningless) for $\epsilon > 1/2$. Thus, the MF approximation predicts, for every admissible λ , both the zero density and a non-zero density solution for $\epsilon \in [0, 1/2]$, while for $\epsilon \geq 1/2$ the sole zero density measure is found. We can thus conclude that, given ϵ , the MF approximation is not able to detect any transition.

As reported in Figure 8, the MF prediction is largely improved by the BA. If ϵ is large enough, two transitions between the zero and the non-zero density are detected. Indeed, there exists an interval of values of λ in which the zero density measure is found as the solution of the iterative equations initialized with the Bernoulli measure, meaning that the associated fixed point in the measure space is stable.

VI. CONCLUSIONS

We have studied the dynamics of a probabilistic cellular automaton obtained as a stochastic mixture of the additive ECA rules 60 and 102. The model provides a nontrivial example of a probabilistic combination of two mirror-symmetric linear automata, whose stochastic dynamics exhibit an absorbing zero stationary state for a finite interval of values of the mixing parameter. The

physics interpretation would be that the competition between the right and left moving rules 60 and 102 leads to the stabilization of an intermediate zero-density phase.

A central result of this work is that standard block approximation schemes fail systematically to reproduce this absorbing stationary state. The failure can be traced to the additive and mirror symmetries of the underlying deterministic rules, which impose global algebraic constraints on the evolution of configurations. Such constraints are not representable within a closure based on finitely many local marginals, and the resulting block approximation equations preserve spurious stationary solutions that do not correspond to invariant measures of the exact stochastic dynamics. This shows that, for probabilistic mixtures of linear cellular automata, mean-field-type closures may yield qualitatively incorrect predictions even in regimes where the exact finite system almost surely reaches an absorbing state.

The contrast with percolation-type PCA, such as the Domany–Kinzel model ([26]), is instructive. In those systems the update rule is monotone: activity can only be generated locally from pre-existing activity, and once a configuration becomes locally inactive it cannot regenerate activity at later times. As a consequence, the long-time behavior is determined by local interactions, and low-order block approximations are sufficient to capture the qualitative structure of the extinction transition.

More generally, our results indicate that approximation schemes based on finite local marginals may be unreliable for stochastic cellular automata whose dynamics are governed by additive or other algebraic symmetries. In such systems, global constraints on configuration space can dominate the long-time behavior, leading to qualitative discrepancies between the exact process and its finite-order closures. Developing approximation methods capable of incorporating such constraints remains an interesting direction for future work.

ACKNOWLEDGMENTS

ENMC thanks GNFM and the PRIN 2022 project “Mathematical Modelling of Heterogeneous Systems (MMHS)”, financed by the European Union - Next Generation EU, CUP B53D23009360006, Project Code 2022MKB7MM, PNRR M4.C2.1.1.

[1] R. Fernandez, P.-Y. Louis, and F.R. Nardi. Overview: PCA models and issues. In P.-Y Louis and F. R. Nardi, editors, *Probabilistic Cellular Automata: theory, applications and future perspectives*, pages 1–30. Springer International Publishing, 2018.

[2] C.A. Valentim, J.A. Rabi, and S.A. David. Cellular automaton model for tumor growth dynamics: virtualization of different scenarios. *Computers in Biology and Medicine*, 153:106481, 2023.

[3] P. Davis. Does new physics lurk inside living matter? *Physics Today*, 73(8):34, 2020.

[4] S. Wolfram. Statistical mechanics of cellular automata. *Rev. Mod. Phys.*, 35:601–644, 1983.

[5] S. Wolfram. Computation theory of cellular automata. *Comm. Math. Phys.*, 96:15–57, 1984.

[6] N. Fatés. Diploid cellular automata: First experiments on the random mixtures of two elementary rules. *Lectures Notes in Computer Science*, 10248:97–108, 2017.

[7] A. Busic, J. Mairesse, and I. Marcovici. Probabilistic cellular automata, invariant measures, and perfect sampling. *Adv. in Appl. Probab.*, 45:960–1980, 2013.

[8] A. Toom. *Contours, convex sets and cellular automata*. IMPA mathematical publications, 2004.

[9] J. Mairesse and I. Marcovici. Around probabilistic cellular automata. *Theoretical Computer Science*, 559:42–72, 2014.

[10] J.R.G. Mendonça. Monte Carlo investigation of the critical behavior of stavskaya’s probabilistic cellular automaton. *Phys. Rev. E*, 83:42–72, 2011.

[11] D. Dhar. Exact solution of a directed-site animals-enumeration problem in three dimensions. *Phys. Rev. Lett.*, 51:853–856, 1983.

[12] S. Wolfram. *A New Kind of Science*. Wolfram Media, Champaign, Illinois, 2002.

[13] E.N.M. Cirillo, G. Lancia, and C. Spitoni. Block approximations for probabilistic mixtures of elementary cellular automata. *Physica A*, 654:130150, 2024.

[14] S. Paul, S. Roy, and S. Das. On convergence of temporally stochastic cellular automata. *Natural Computing*, 25(1):5, 2026.

[15] J.R. Mendonça and M.J. de Oliveira. An extinction-survival-type phase transition in the probabilistic cellular automaton p182–q200. *Journal of Physics A: Mathematical and Theoretical*, 44(15):155001, 2011.

[16] N. Fatès. Asynchronism induces second order phase transitions in elementary cellular automata. *Journal of Cellular Automata*, 2008.

[17] E.N.M. Cirillo, F.R. Nardi, and C. Spitoni. Phase transitions in random mixtures of elementary cellular automata. *Physica A*, 573:125942, 2021.

[18] H. Fukś and N. Fatès. Local structure approximation as a predictor of second order phase transitions in asynchronous cellular automata. *Natural computing*, 14:507–522, 2015.

[19] H.A. Gutowitz, J.D. Victor, and B.W. Knight. Local structure theory for cellular automata. *Physica D*, 28:18–48, 1987.

[20] H.A. Gutowitz and J.D. Victor. Local structure theory in more than one dimension. *Complex Systems*, 1:57–68, 1987.

[21] R. Kikuchi. Superposition approximation and natural iteration calculation in cluster–variation method. *J. Chem. Phys.*, 60:1071–1080, 1974.

[22] A. Pelizzola. Cluster variation method in statistical physics and probabilistic graphical models. *J. Phys. A: Math. Gen.*, 38:R309, 2005.

[23] E.N.M. Cirillo, G. Gonnella, and A. Pelizzola. Folding transition of the triangular lattice in a discrete three-dimensional space. *Physical Review E*, 53:3253, 1996.

[24] E.N.M. Cirillo, G. Gonnella, M. Troccoli, and A. Marian. Correlation functions by cluster variation method for ising model with nn, nnn and plaquette interactions. *Journal of Statistical Physics*, 94:67–89, 1999.

[25] H. Fukś. Construction of local structure maps for cellular automata. *Journal of Cellular Automata*, 7, 2012.

[26] E. Domany and W. Kinzel. Equivalence of cellular automata to ising models and directed percolation. *Physical review letters*, 53(4):311, 1984.